J Mol Model (2013) 19:4545–4554
DOI 10.1007/s00894-013-1968-8

ORIGINAL PAPER

Nickel/zinc-catalyzed decarbonylative addition of anhydrides to alkynes: A DFT study

Qingxi Meng · Ming Li

Received: 16 December 2012 / Accepted: 29 July 2013 / Published online: 17 August 2013

Abstract Density functional theory (DFT) was used to investigate the nickel- or nickel(0)/zinc- catalyzed decarbonylative addition of phthalic anhydrides to alkynes. All intermediates and transition states were optimized completely at the B3LYP/6-31+G(d,p) level. Calculated results indicated that the decarbonylative addition of phthalic anhydrides to alkynes was exergonic, and the total free energy released was −87.6 kJ mol^{-1}. In the five-coordinated complexes **M4a** and **M4b**, the insertion reaction of alkynes into the Ni-C bond occurred prior to that into the Ni-O bond. The nickel(0)/zinc-catalyzed decarbonylative addition was much more dominant than the nickel-catalyzed one in whole catalytic decarbonylative addition. The reaction channel **CA→M1'→T1'→M2'→T2'→M3a'→M4a'→T3a1'→M5a1' → T4a1'→M6a'→P** was the most favorable among all reaction pathways of the nickel- or nickel(0)/zinc- catalyzed decarbonylative addition of phthalic anhydrides to alkynes. And the alkyne insertion reaction was the rate-determining step for this channel. The additive $ZnCl_2$ had a significant effect, and it might change greatly the electron and geometry structures of those intermediates and transition states. On the whole, the solvent effect decreased the free energy barriers.

Keywords Alkynes · Anhydrides · Nickel catalyst · Decarbonylative addition · DFT · Reaction mechanism · $ZnCl_2$

Introduction

The insertion reaction of an unsaturated C-C bond into a C-O bond of an oxacyclic compound catalyzed by transition metal complexes is a useful transformation, because more complicated oxacyclic compounds are attained, e.g., isocoumarin which displays a wide range of biological activities [1, 2]. Isocoumarin could be synthesized by many transition metals catalysts [3–6]. Recently, Kurahashi et al. [6] reported the nickel(0)-catalyzed decarbonylative addition of phthalic anhydrides (**R1**) to alkynes (**R2**) to form isocoumarin (**P**), as illustrated in Scheme 1. They described the decarbonylative addition with 10 mol% of $Ni(cod)_2$ (cod = 1,5-cyclooctadiene) and 40 mol% of PMe_3 led to isocoumarin in 12 % yield. However, on addition of 20 mol% of the Lewis acids as additive (e.g., $ZnCl_2$, $Zn(OTf)_2$ (OTf = triflate), $ZnBr_2$, ZnI_2, BPh_3 (Ph = phenyl), LiCl, et al.), the reaction proceeded smoothly to furnish isocoumarin in more than 70 % isolated yield. And $ZnCl_2$ gave the best yield of the product, 96 % isolated yield.

Kurahashi et al. also suggested a likely mechanism outlined in Scheme 2. The catalytic cycle should consist of the oxidative addition of an anhydride O-CO bond to nickel [7–9], subsequent decarbonylation, and the coordination of alkyne to give the nickel(II) intermediate **A**. And then the alkyne would insert into the aryl-nickel bond to give the nickelacycle intermediate **B**, which would undergo the reductive elimination to form isocoumarin and regenerate the catalyst. The origin of the effect of $ZnCl_2$ was likely to result from the coordination of a Lewis acid to a carbonyl group, which might generate electron-poor alkenylnickel through a conjugated system.

Electronic supplementary material The online version of this article (doi:10.1007/s00894-013-1968-8) contains supplementary material, which is available to authorized users.

Q. Meng · M. Li (✉)
College of Chemistry and Chemical Engineering, Southwest University, Chongqing 400715, People's Republic of China
e-mail: liming@swu.edu.cn

Q. Meng (✉)
College of Chemistry and Material Science, Shandong Agricultural University, Taian, Shandong 271018, People's Republic of China
e-mail: qingxim@sdau.edu.cn

Scheme 1 The nickel-catalyzed decarbonylative addition of phthalic anhydrides to alkynes

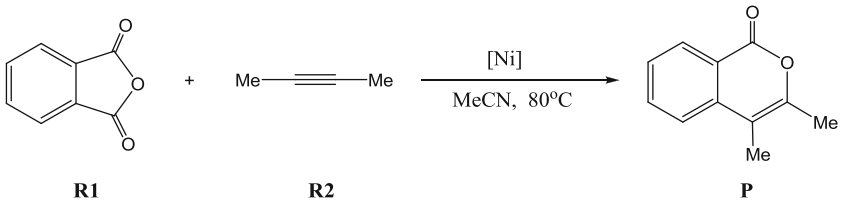

In order to understand the reaction mechanism of the nickel(0)-catalyzed decarbonylative addition of anhydrides to alkynes to form isocoumarin in detail, the decarbonylative addition of phthalic anhydrides to alkynes catalyzed by the catalysts nickel(0)/PMe_3 with $ZnCl_2$ was studied in the present work. Specifically, the present study would focus on: (1) the energitics of the overall catalytic pathways in the nickel(0)-catalyzed decarbonylative addition, (2) the energitics of the catalytic pathways in the nickel(0)/zinc-catalyzed decarbonylative addition, (3) the structural features of intermediates and transition states involved, (4) the possible insertion reaction channels of the alkyne into the aryl-nickel bond, (5) the effect of $ZnCl_2$, and (6) the effect of the solvent in the reaction mechanism.

Computational details

All calculations were carried out with the Gaussian 03 programs [10]. The geometries of all the species were fully optimized by using density functional theory (DFT) [11] of B3LYP method [12, 13] with the 6-31+G(d,p) basis set for all the atoms. Frequency calculations were performed to confirm each stationary point to be either a minimum (**M**) or a transition structure (**T**). The transition states were verified by intrinsic reaction coordinate (IRC) [14] calculations and by animating the negative eigenvector coordinates with a visualization program (Molekel 4.3) [15, 16]. In addition, the bonding characteristics were analyzed by the natural bond orbital (NBO) theory [17–20]. NBO analysis was performed by utilizing NBO5.0 code [21]. Based on the gas phase optimized geometry for each species, the solvent effects of CH_3CN (acetonitrile, ε=36.64) were studied by performing a self-consistent reaction field (SCRF) [22, 23] of polarizable continuum model (PCM) [24] approach at the same computational level using the default parameters except the temperature (353.15 K was used).

Furthermore, the electron densities ρ at the bond critical points (BCPs) or the ring critical points (RCPs) for some species were calculated by employing the AIM 2000 program package [25, 26].

Results and discussion

The possible reaction mechanisms of the nickel(0)-catalyzed decarbonylative addition were outlined in Scheme 3. The relative gas phase free energies ΔG, enthalpies ΔH, zero-point energy (ZPE) corrected electronic energies ΔE, and absolute entropies S were summarized in Tables S1-4. Unless otherwise noted, the discussed energies were the gas phase free energies ΔG in the following discussions.

The complexation reaction of phthalic anhydrides and $Ni(PMe_3)_4$

The complexation reaction of $Ni(PMe_3)_4$ with phthalic anhydrides resulted in two possible complexes **M1** and **M1-1**: the first one was formed through a synergic pπ-dπ back-donation bond between nickel and C1-O1 double bond, while the latter was formed by a coordinate bond between nickel and the oxygen atom O1. The occupied π bonding orbital ($\pi_{C1\text{-}O1}$) acted on the empty hybridized orbital of nickel leading to a σ coordinate bond; on the other hand, the occupied d orbital (d_{xy}, d_{xz}, d_{yz}) of nickel acted on the empty π* antibonding orbital ($\pi^*_{C1\text{-}O1}$) leading to a π back-donation bond. Obviously, the formation of the synergic pπ-dπ back-donation bond lowered the system's energy and made the nickel complex **M1** more stable.

The free energy of **M1** was lower than **M1-1** by 61.5 kJ mol^{-1}, so **M1** was more stable suggesting that it was more possible to exist. NBO energy of the C1-O2 bond in **M1** was higher than phthalic anhydride by 298.0 kJ mol^{-1}, while NBO energy of the C1-O2 bond in **M1-1** was higher than phthalic anhydride by 73.6 kJ mol^{-1}. Hence, in **M1**, the formation of the pπ-dπ back-donation bond weakened and activated the C1-O2 bond, which would result in the oxidative addition reaction of phthalic anhydride.

Scheme 2 Plausible mechanism for the nickel-zinc-catalyzed decarbonylative addition of phthalic anhydrides to alkynes

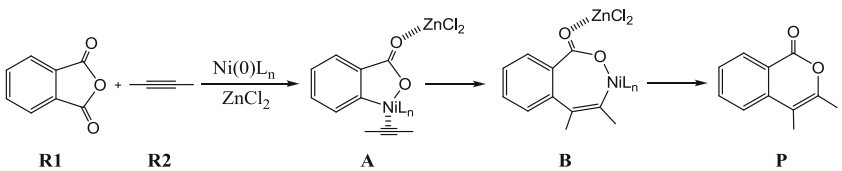

Scheme 3 Possible reaction mechanism of the nickel-catalyzed decarbonylative addition of phthalic anhydrides to alkynes

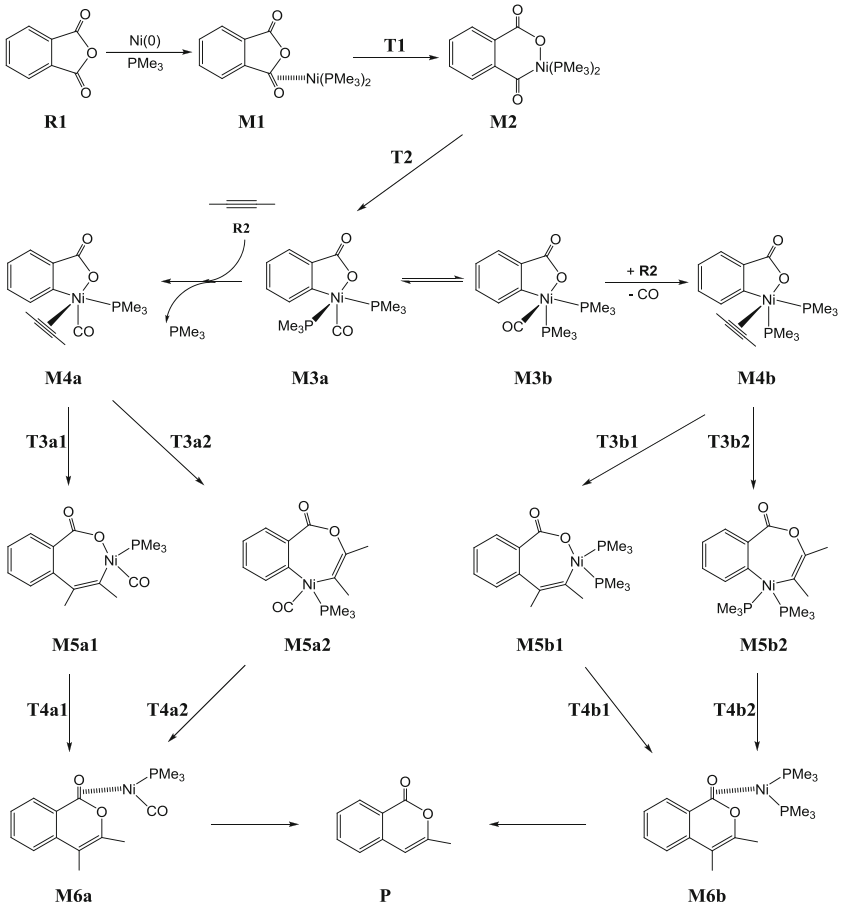

Nickel(0)-catalyzed decarbonylative addition without $ZnCl_2$

Figure 1 showed the potential energy hypersurface for the most favorable pathway in the nickel-catalyzed decarbonylative addition of phthalic anhydrides to alkynes to form isocoumarin. The oxidative addition reaction of phthalic anhydride went through the C1-O2 activation transition state **T1** with a free energy of activation of 55.3 kJ mol^{-1} leading to the four-coordinate nickel(II) complex **M2**. This species then underwent a decarbonylation through the

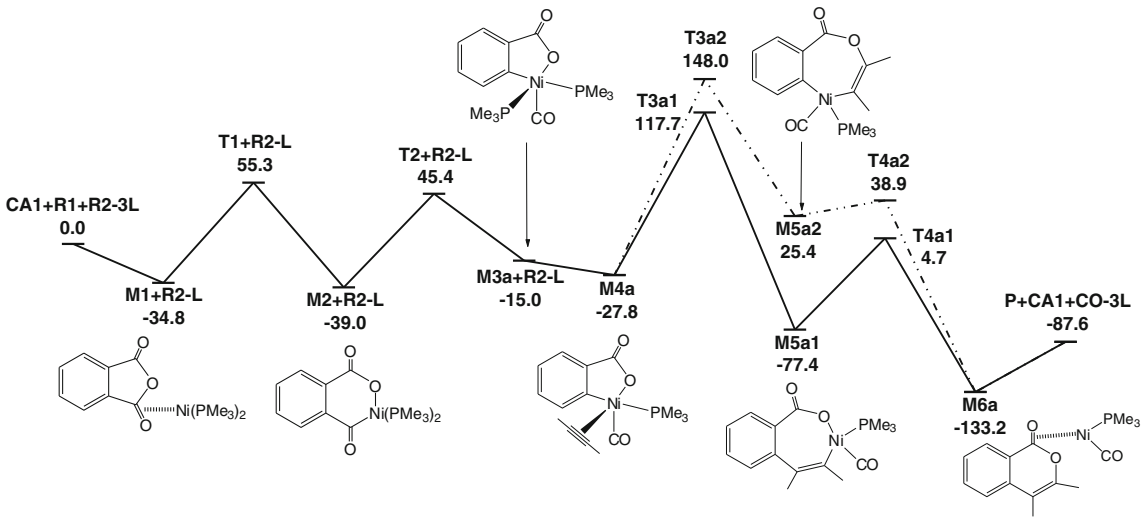

Fig. 1 Free energy profiles for the most favorable path (**a**) in the nickel-catalyzed decarbonylative addition of phthalic anhydrides to alkynes. (The free energies ΔG were given in kJ mol^{-1}, **CA1** = $Ni(PMe_3)_4$, **L** = PMe_3.)

transition state **T2** with a free energy of activation of 45.4 kJ mol^{-1} to give the five-coordinate complex **M3a**. The coordination reaction of an alkyne (**R2**) to **M3a** generated the five-coordinate nickel complex **M4a**, releasing a coordinated ligand PMe_3. Next, intermediate **M4a** went through an alkyne insertion reaction via the transition states **T3a1** and **T3a2** with the free energies of activation of 117.7 and 148.0 kJ mol^{-1}, leading to the nickelacycle complex **M5a1** and **M5a2**, respectively. Finally, intermediates **M5a1** and **M5a2** underwent the reductive elimination reaction, respectively, via the transition states **T4a1** and **T4a2** with the free energies of activation of 4.7 and 38.9 kJ mol^{-1} to form the nickel-isocoumarin complex **M6a** releasing the product **P**. Obviously, the transition states **T3a1** and **T3a2** were the highest stationary points in the process of forming the isocoumarin **P**. Hence, the alkyne insertion reaction was the rate-determining step for these pathways in the nickel-catalyzed decarbonylative addition. As shown in Scheme 3 and Fig. S1, the alkyne insertion reaction had two possible reaction channels: C6 attacking C2 was denoted "**a1**", while C6 attacking O2 was denoted "**a2**". It was evident that the reaction channel "**a1**" was more dominant than "**a2**" (i.e., the insertion reaction of alkynes into the Ni-C bond occurred prior to that into the Ni-O bond), because the free energy of activation of **T3a1** was lower than **T3a2** by 30.3 kJ mol^{-1}.

In the four-coordinate complex **M2**, Ni, C1, O2 and two phosphorus atoms were nearly coplanar, and there was a Ni-C1-C2-C3-C4-O2 six-membered ring and the electron density ρ of the RCP is 0.016 e·$Å^{-3}$. NBO analysis of **M2** indicated that the Ni-C1 and Ni-O2 bonds showed strong single-bonded character, so the synergic pπ-dπ back-donation bond between nickel and $\pi_{C1\text{-}O1}$ was disruptive. In the decarbonylation, the distances between Ni and C1 and C2, $d_{Ni\text{-}C1}$ and $d_{Ni\text{-}C2}$, were 1.723 and 2.076 Å, while $d_{C1\text{-}C2}$ was 1.748 Å, indicating a significant interaction between Ni and C2 occurred, conversely the C1-C2 bond was weakened considerably, as demonstrated by analyzing the changes of Wiberg bond orders P_{ij} and electron density ρ at the BCPs (e.g., C1-C2 bond, P_{ij}, **M2**: 0.967→**T2**: 0.793→**M3a**: 0.100; ρ, **M2**: 0.262→**T2**: 0.150→**M3a**: 0.000 e·$Å^{-3}$). **M3a** was a five-coordinate complex, and involved a Ni-C2-C3-C4-O2 five-membered ring and the electron density of the RCP was 0.028 e·$Å^{-3}$. The Ni-C1, Ni-C2, Ni-O2, and two Ni-P bonds are, respectively, 1.750, 1.947, 1.903, 2.282 and 2.633 Å. And there was again the pπ-dπ back-donation bond between nickel and carbonyl. Obviously, of the coordinated ligands CO and two PMe_3, it was easiest that an alkyne substituted for PMe_3 with the Ni-P bond of 2.633 Å to give the complex **M4a**. The alkyne insertion reaction had two possible reaction channels, and the corresponding transition states were **T3a1** and **T3a2**, respectively. **T3a1** involved a Ni-C2-C3-C4-O2 five-membered ring and a Ni-C2-C6-C7 four-membered ring, and the electron densities of the RCPs were 0.026 and 0.075 e·$Å^{-3}$. **T3a2** involved a Ni-C2-C3-C4-O2 five-membered ring and a Ni-O2-C6-C7 four-membered ring, and the electron densities of the RCPs were 0.023 and 0.030 e·$Å^{-3}$. **M5a1** involved a Ni-C7-C6-C2-C3-C4-O2 seven-membered ring, and **M5a2** involved a Ni-C2-C3-C4-O2-C6-C7 seven-membered ring. As presented in Fig. 1 and Table S1, the free energy of **M5a1** was lower than **M5a2** by 102.8 kJ mol^{-1}. The steric and structural hindrance between the ringed structure and PMe_3 of **M5a1** was much weaker than **M5a2**, and there were three hydrogen bonds of $O(CO_2)$…H-C(PMe_3) (2.673, 2.827, and 3.277 Å) in **M5a1** which was much stronger than **M5a2** with a hydrogen bond of $O(CO_2)$…H-C(PMe_3) (2.881 Å) Fig. 2.

In addition, the other two reaction pathways were shown in Scheme 3 and Fig. S2. Intermediate **M3a** isomerized to the complex **M3b** which coordinated to alkynes to give the complex **M4b** releasing CO. Being similar to **M4a**, the alkyne insertion reaction of **M4b** had again two possible reaction channels.

By contrast, several results for these alternative reaction channels in the nickel-catalyzed decarbonylative addition could be summarized as follows: (1) The alkyne insertion reaction was the rate-determining step, because the transition states **T3** were the highest stationary points in every reaction channel (Table S1 and S2, Supporting information). (2) In the complexes **M4a** and **M4b**, the insertion reaction of alkynes into the Ni-C bond occurred prior to that into the Ni-O bond. (3) The complex **M3a** possessed better stability than **M3b**, so the isomerization reaction of **M3a** to **M3b** would be difficult to achieve. (4) The complex **M4a** was suggested more possible to exist than **M4b**, because of the free energy of **M4a** being lower than **M4b** by 99.3 kJ mol^{-1}. (5) The step **M3a**→**M4a** (i.e., the coordination reaction of alkynes) was exothermic by 12.8 kJ mol^{-1}, while the step **M3b**→**M4b** was endothermic by 58.0 kJ mol^{-1}. (6) In the coordination reaction, the alkynes found it easier to substitute for PMe_3 than carbonyl. (7) The reaction channel **CA**→**M1**→**T1**→**M2**→**T2**→**M3a**→ **M4a**→**T3a1**→**M5a1**→**T4a1**→**M6a**→**P** was the most favorable in the nickel-catalyzed decarbonylative addition (Fig. 1).

Nickel(0)/znic-catalyzed decarbonylative addition

Figure 3 showed the potential energy hypersurface for the nickel/zinc-catalyzed decarbonylative addition of phthalic anhydrides to alkynes to form isocoumarin. The coordination reaction of phthalic anhydride with $Ni(PMe_3)_4$ and $ZnCl_2$ (Ni:Zn=1:2) led to the nickel(0)-zinc(II)-anhydride complex **M1'**. This species underwent the oxidative addition reaction of anhydride, via the transition state **T1'** with a free energy of activation of −17.3 kJ mol^{-1} giving the complex **M2'**. And intermediate **M2'** then went through a decarbonylation through the transition state **T2'** with a free energy of activation

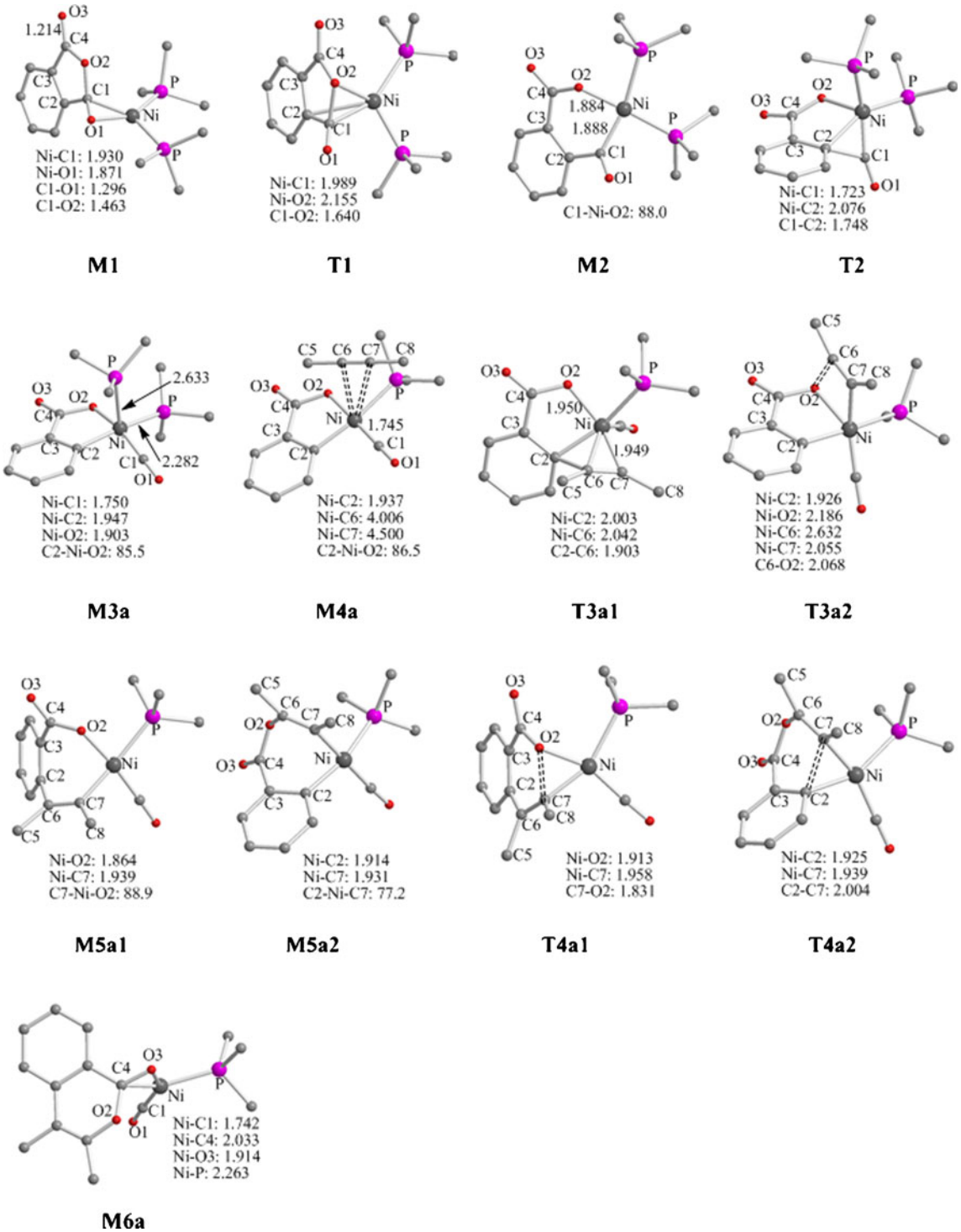

Fig. 2 Intermediates and transition states of the most favorable path (**a**) in the nickel-catalyzed decarbonylative addition of phthalic anhydrides to alkynes. (Some bond lengths were given in Å, hydrogen atoms were omitted for clarity)

of −41.3 kJ mol^{-1} to form a five-coordinate complex **M3a'**. Next, the complexation reaction of alkyne and **M3a'** generated a five-coordinate complex **M4a'** releasing a coordinated ligand PMe_3. Intermediate **M4a'** subsequently underwent an alkyne insertion reaction, respectively, via the transition states **T3a1'** and **T3a2'** with the free energies of activation of 60.1 and 84.3 kJ mol^{-1}, resulting in the complex **M5a1'** and **M5a2'**. Finally, intermediates **M5a1'** and **M5a2'** went through the reductive elimination reaction via the transition states **T4a1'** and **T4a2'** with the free energies of activation of

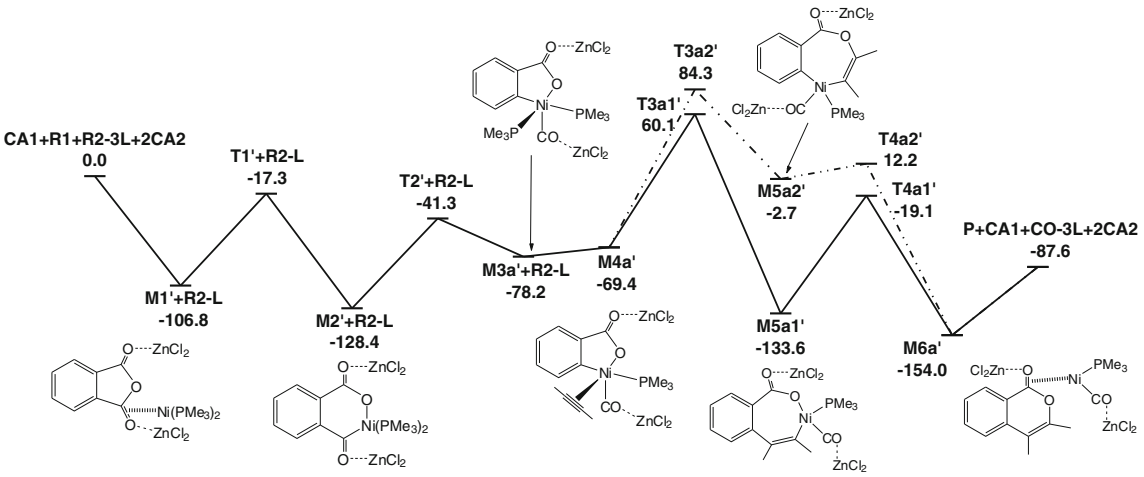

Fig. 3 Free energy profiles for the nickel-zinc-catalyzed decarbonylative addition of phthalic anhydrides to alkynes. (The free energies ΔG were given in kJ mol^{-1}, **CA1** = $Ni(PMe_3)_4$, **CA2** = $ZnCl_2$, **L** = PMe_3.)

−19.1 and 12.2 kJ mol^{-1} to give the complex **M6a'** releasing isocoumarin **P**. It was clear that the transition states **T3a1'** and **T3a2'** were the highest stationary point in the process of forming the isocoumarin. Therefore, the alkyne insertion reaction was the rate-determining step for these pathways in the nickel/zinc-catalyzed decarbonylative addition. The free energy of activation of **T3a1'** was lower than **T3a2'** by 24.2 kJ mol^{-1}, so the reaction channel "**a1**" was more dominant than "**a2**", indicating that the insertion reaction of alkynes into the Ni-C bond occurred prior to that into the Ni-O bond. These results agreed with those discussed above in the nickel-catalyzed decarbonylative addition without $ZnCl_2$.

Four ligands of the four-coordinate complex **M2'** were not coplanar, which was different from **M2**. As illustrated in NBO analysis, the Ni-C1 bond of **M2'** showed strong single-bonded character, and the NBO energy was −1252.7 kJ mol^{-1} which was lower than **M2** by 172.5 kJ mol^{-1}. And there was a Ni-C1-C2-C3-C4-O2 six-membered ring (Fig. 4), and the electron density of the RCP was 0.015 e·Å^{-3}. Transition state **T3a1'** involved a Ni-C2-C3-C4-O2 five-membered ring and a Ni-C2-C6-C7 four-membered ring, and the electron densities of the RCPs were 0.025 and 0.068 e·Å^{-3}, respectively. The atomic polar tensors (APT) charges of carbon atoms of the C2-C6 bond were +0.258 and +0.173. The high stabilization energies of 104.4, 160.4, and 199.4 kJ mol^{-1} for the $\sigma_{Ni\text{-}C7} \rightarrow \sigma^*_{C2\text{-}C6}$, $\sigma_{C2\text{-}C6} \rightarrow (4d)^*_{Ni}$, and $\sigma_{C2\text{-}C6} \rightarrow \sigma^*_{Ni\text{-}C7}$ in **T3a1'** (Table S6, Supporting information), which was obtained from the second-order perturbation analysis of donor-acceptor interactions in the NBO analysis and used to estimate the strengths of the donor-acceptor interactions of the NBOs, revealed the strong interaction between $\sigma_{Ni\text{-}C7}$ and $\sigma^*_{C2\text{-}C6}$, $\sigma_{C2\text{-}C6}$ and $(4d)^*_{Ni}$ or $\sigma^*_{Ni\text{-}C7}$, and the electron transfer tendency from $\sigma_{Ni\text{-}C7}$ to $\sigma^*_{C2\text{-}C6}$, $\sigma_{C2\text{-}C6}$ to $(4d)^*_{Ni}$ and $\sigma^*_{Ni\text{-}C7}$. Furthermore, Table S6 suggested the electron transfer tendency form $(2s)_{C1}$, $(2p)_{O2}$, and $(3s)_P$ to $(4d)^*_{Ni}$ and $\sigma^*_{Ni\text{-}C7}$. These results indicated that the alkyne insertion reaction was promoted. Figure 3 showed that the free energy of **M5a1'** was lower than **M5a2'** by 130.9 kJ mol^{-1}. The steric and structural hindrance between the ringed structure, $CO(ZnCl_2)$, and PMe_3 of **M5a1'** was much weaker than **M5a2'**, and there were four hydrogen bonds of Cl…H-C(PMe_3) (2.881 and 2.917 Å) and O(CO_2)…H-C(PMe_3) (3.029 and 3.169 Å) in **M5a1'** which was much stronger than **M5a2'** with two hydrogen bonds of Cl…H-C(PMe_3) (2.990 and 3.152 Å).

The effect of $ZnCl_2$

Kurahashi et al. showed that nickel(0)-catalyzed decarbonylative addition reaction of anhydrides to alkynes proceeded to furnish isocoumarin in 96 % yield by adding $ZnCl_2$ as additive, however, in only 12 % yield without any additive. And they speculated that the origin of the effect of $ZnCl_2$ was likely to result from the coordination of a Lewis acid to a carbonyl group, which might generate electron-poor alkenylnicjel through a conjugated system. Therefore, to understand the effect of $ZnCl_2$, we studied theoretically the reaction pathways of the nickel(0)- and nickel(0)/zinc- catalyzed decarbonylative addition of phthalic anhydrides to alkynes, respectively.

As discussed above, the reaction channel **CA→M1→T1→M2→T2→M3a→M4a →T3a1→M5a1→T4a1→M6a→P** was the most favorable among all of the reaction pathways of the nickel-catalyzed decarbonylative addition, and the alkyne insertion reaction was the rate-determining step and the transition state **T3a1** with the free energy of activation of 117.7 kJ mol^{-1} was the highest stationary point in this channel. In the nickel(0)/zinc-catalyzed decarbonylative addition, the reaction channel **CA→ M1'→T1'→M2'→T2'→M3a'→M4a'→T3a1'→M5a1'→T4a1'→M6a'→P** was the most favorable, and the alkyne

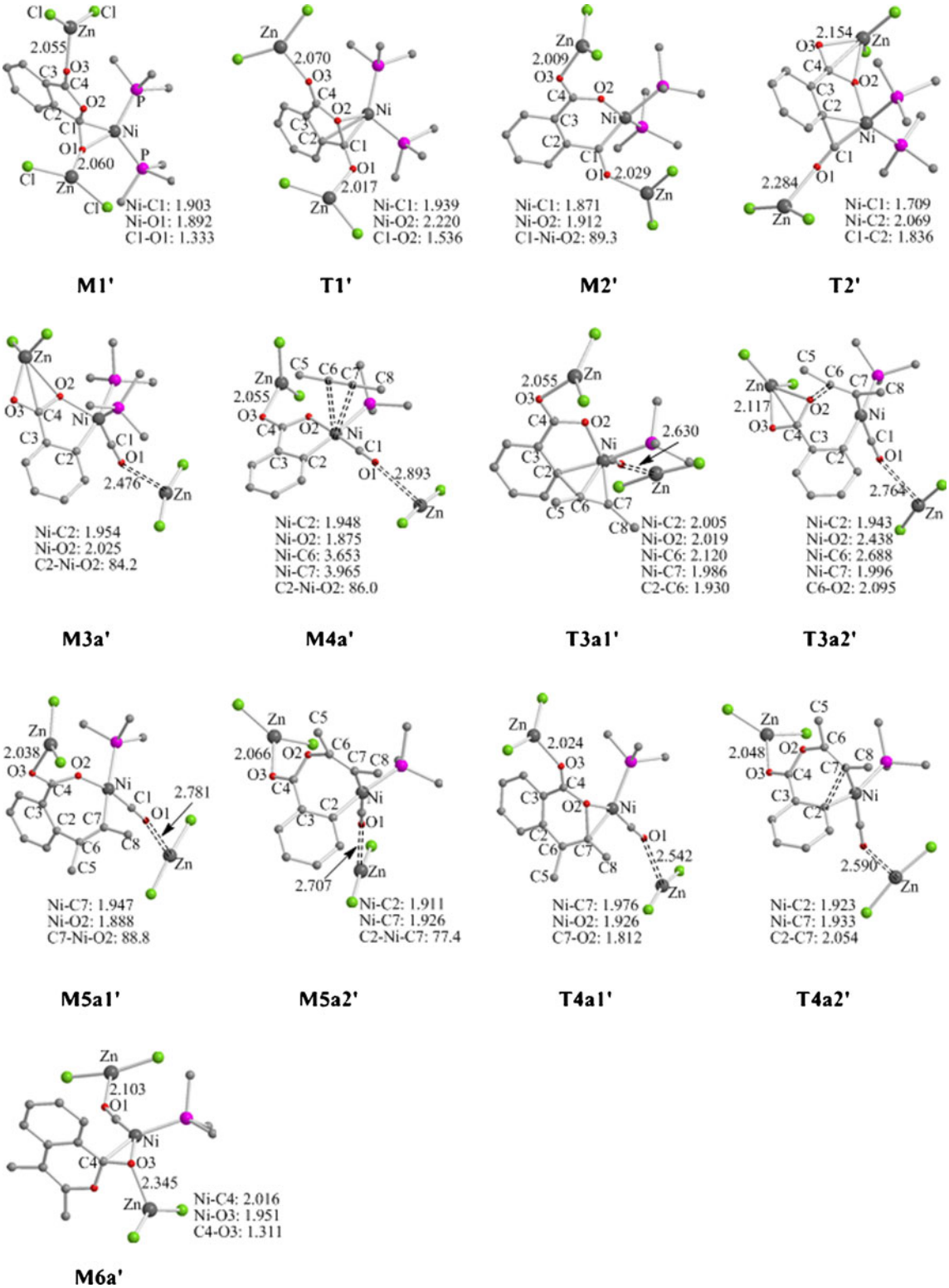

Fig. 4 Intermediates and transition states of the nickel-zinc-catalyzed decarbonylative addition of phthalic anhydrides to alkynes. (Some bond lengths were given in Å, hydrogen atoms were omitted for clarity)

insertion reaction was again the rate-determining step and the transition state **T3a1'** with the free energy of activation of 60.1 kJ mol^{-1} was the highest stationary point in this channel. Clearly, the free energy of **T3a1'** was lower than **T3a1** by 57.6 kJ mol^{-1}, so the nickel(0)/zinc-catalyzed decarbonylative addition was much more dominant than the nickel-catalyzed

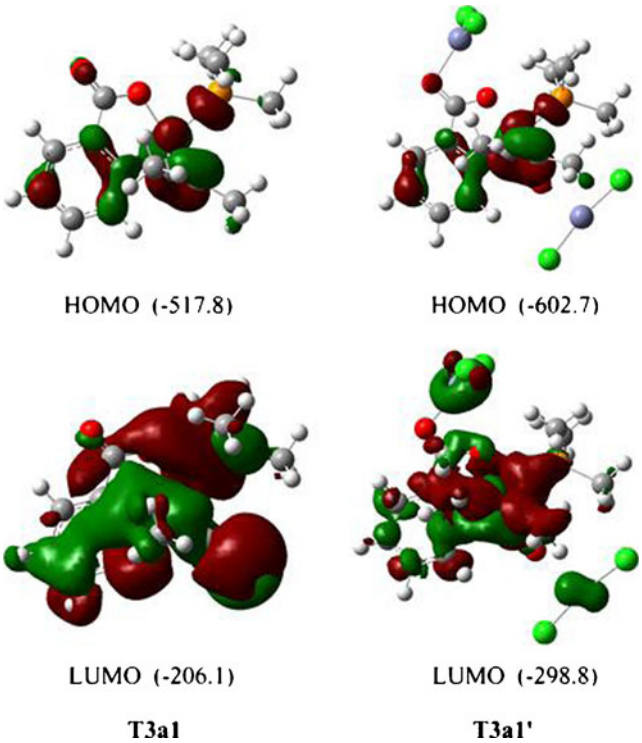

Fig. 5 The HOMOs and LUMOs of **T3a1** and **T3a1'**. (Energies were given in kJ mol^{-1})

one. As illustrated in Fig. 5, the HOMO of **T3a1'** seemed similar to **T3a1**, while the orbital energy was lower by 84.9 kJ mol^{-1}; The LUMO of **T3a1'** was greatly different from **T3a1** and related to $ZnCl_2$. Hence, the additive $ZnCl_2$ changed greatly the electron and geometry structures of the intermediates and transition states. Comparing and contrasting Fig. 1 with Fig. 3, we found that the free energies of all the intermediates and transition states were decreased greatly by adding $ZnCl_2$ as additive, implying that the effect of $ZnCl_2$ was significant.

However, could the additive of $ZnCl_2$ change the reaction channel? So, we also studied the other two reaction paths: (1) the complexation reaction of alkyne to zinc of **M3a'** generated a five-coordinate complex **M4c'**, and then **M4c'** underwent an alkyne insertion reaction via a transition state **T3c'** with the free energy of activation of 106.6 kJ mol^{-1} to give the complex **M5c'**; (2) the isomerization reaction of **M4a'** resulted in a four-coordinate complex **M4d'** where the alkyne coordinated with zinc, and **M4d'** subsequently underwent an alkyne insertion reaction via a transition state **T3d'** with the free energy of activation of 72.8 kJ mol^{-1} to form the complex **M5d'**. The optimized structures of these transition states and intermediates were shown in Fig. S3, and the relative free energies were summarized in Table S4. Clearly, the free energies of two transition states were higher than **T3a1'**. The reaction free energy barriers of the transition states **T3a1'**, **T3c'**, and **T3d'** were 129.5, 179.0, and 163.3 kJ mol^{-1}, respectively. And the free energy of **T3a1'** was the lowest, so the other two reaction paths discussed above were minor in the nickel(0)/zinc-catalyzed decarbonylative addition of phthalic anhydrides to alkynes. Therefore, the additive $ZnCl_2$ could not change the reaction channel, and it changed greatly only the electron and geometry structures of those intermediates and transition states.

Overview of the reaction mechanism

As discussed above, the reaction mechanisms of the nickel(0)- and nickel(0)/zinc- catalyzed decarbonylative addition were studied. Calculated results indicated that the decarbonylative addition was exergonic, and the total released free energy was −87.6 kJ mol^{-1}.

The complex **M3a** possessed better stability than **M3b**, and the complex **M4a** was suggested more possible to exist than **M4b**. The alkyne found it is easier to substitute for PMe_3 than carbonyl in the coordination reaction. In the complexes **M4a** and **M4b**, the insertion reaction of alkynes into the Ni-C bond occurred prior to that into the Ni-O bond. The reaction channel **CA→M1→T1→M2→T2→M3a→M4a→T3a1→ M5a1→T4a1→M6a→P** was the most favorable in the nickel-catalyzed decarbonylative addition, and the alkyne insertion reaction was the rate-determining step. In the nickel(0)/zinc-catalyzed decarbonylative addition, the reaction channel **CA→M1'→T1'→M2'→T2'→M3a'→M4a'→T3a1'→M5a1'→T4a1'→M6a'→P** was the most favorable, and the alkyne insertion reaction was again the rate-determining step. In whole catalytic decarbonylative addition of phthalic anhydrides to alkynes, the nickel(0)/zinc-catalyzed one is much more dominant than nickel-catalyzed one. Therefore, the reaction channel **CA→M1'→T1'→ M2'→T2'→ M3a'→M4a'→T3a1'→M5a1'→T4a1'→ M6a'→P** was the most favorable among all the catalytic decarbonylative addition of phthalic anhydrides to alkynes.

The additive $ZnCl_2$ had a significant effect, and it decreased greatly the free energies of all the intermediates and transition states. And it could not change the reaction channel, and it changed greatly only the electron and geometry structures of those intermediates and transition states.

The effect the solvent

To evaluate the solvent effect for acetonitrile (CH_3CN, ε=36.64), single-point computations had been performed at the B3LYP/6-31+G(d,p) level by the PCM model using the default parameters except the temperature (353.15 Kelvin was used) [6]. The relative free energies ΔG(sol) for the stationary points on the most favorable channel in the Ni(0)-Zn(II)-catalyzed decarbonylative addition were summarized in Table S5. The relative free energy barrier $\Delta G^{\neq}$(sol) of the transition states **T3a1'** was 95.3 kJ mol^{-1}, which was 34.2 kJ

mol^{-1} lower than the energy barrier ΔG (in gas phase). Therefore, in general, the solvation effect was remarkable, and it greatly decreased the free energy barriers.

Conclusions

In summary, the reaction mechanisms of the nickel- or nickel(0)/zinc- catalyzed decarbonylative addition of phthalic anhydrides to alkynes were explored computationally using DFT. Calculated results indicated that the decarbonylative addition of phthalic anhydrides to alkynes was exergonic, and the total released free energy was −87.6 kJ mol^{-1}. The complex **M3a** possessed better stability than **M3b**, and the complex **M4a** was suggested more possible to exist than **M4b**. The alkyne found it is easier to substitute for PMe_3 than carbonyl in the coordination reaction. In the complexes **M4a** and **M4b**, the insertion reaction of alkynes into the Ni-C bond occurred prior to that into the Ni-O bond.

The nickel(0)/zinc-catalyzed decarbonylative addition is much more dominant than nickel-catalyzed one in whole catalytic reaction. The reaction channel **CA→M1'→ T1'→ M2'→T2'→M3a'→M4a'→T3a1'→M5a1'→T4a1'→ M6a'→P** was the most favorable among all the reaction pathways of the nickel- or nickel(0)/zinc- catalyzed decarbonylation addition. And the alkyne insertion reaction was the rate-determining step for this channel.

The additive $ZnCl_2$ had a significant effect, and it decreased greatly the free energies of all the intermediates and transition states. However, it could not change the reaction channel, the additive $ZnCl_2$ changed greatly the electron and geometry structures of those intermediates and transition states. On the whole, the solvation effect was remarkable, and it greatly decreased the free energy barriers.

Acknowledgments This work was supported by the Key Project of Science and Technology of the Ministry of Education, P. R. (grant No. 104263), Natural Science Foundation of Chongqing City, P. R. (grant No. CSTC-2004BA4024). Contract grant sponsor: Science and Technology of the Ministry of Education, People's Republic of China (NO: 104263); Natural Science Foundation of Chongqing City, P. R. (No: CSTC-2004BA4024).

References

1. Agata N, Nogi H, Milhollen M, Kharbanda S, Kufe D (2004) 2-(8-hydroxy-6-methoxy-1-oxo -1H-2-benzopyran-3-yl)propionic acid, a small molecule isocoumarin, potentiates dexamethasone-induced apoptosis of human multiple myeloma mells. Cancer Res 64:8512–8516
2. Pochet L, Frédérick R, Masereel B (2004) Coumarin and isocoumarin as serine protease inhibitors. Curr Pharm Design 10:3781–3796
3. Fukuyama T, Higashibeppu Y, Yamaura R, Ryu I (2007) Complex α–pyrones synthesized by a gold-catalyzed coupling reaction. Org Lett 9:587–589
4. Luo T, Schreiber SL (2007) Complex α-pyrones synthesized by a gold-catalyzed coupling reaction. Angew Chem Int Ed 46:8250–8253
5. Woo JCS, Walker SD, Faul MM (2007) Preparation and decarboxylative rearrangement of (Z)-enyne esters. Tetrahedron Lett 48:5679–5682
6. Kajita Y, Kurahashi T, Matsubara S (2008) Nickel-catalyzed decarbonylative addition of anhydrides to alkynes. J Am Chem Soc 130:17226–17227
7. Fischer R, Walther D, Kempe R, Sieler J, Schönecker B (1993) Metallacyclische acyl-carboxylate des nickels: Reaktivität der acylgruppe und synthesepotential bei kreuzkopplungsreaktionen mit alkylhalogeniden. J Organomet Chem 447:131–136
8. O'Brien EM, Bercot EA, Rovis T (2003) Decarbonylative Cross-coupling of cyclic anhydrides: introducing stereochemistry at an sp3 carbon in the cross-coupling event. J Am Chem Soc 125:10498–10499
9. Johnson JB, Bercot EA, Rowley JM, Coates GW, Rovis T (2007) Ligand-dependent catalytic cycle and role of styrene in nickel-catalyzed anhydride cross-coupling: evidence for turnover-limiting reductive elimination. J Am Chem Soc 129:2718–2725
10. Frisch MJ, Trucks GW, Schlegel HB, Scuseria GE, Robb MA, Cheeseman JR, Montgomery JA, Vreven JT, Kudin KN, Burant JC, Millam JM, Iyengar SS, Tomasi J, Barone V, Mennucci B, Cossi M, Scalmani G, Rega N, Petersson GA, Nakatsuji H, Hada M, Ehara M, Toyota K, Fukuda R, Hasegawa J, Ishida M, Nakajima T, Honda Y, Kitao O, Nakai H, Klene M, Li X, Knox JE, Hratchian HP, Cross JB, Adamo C, Jaramillo J, Gomperts R, Stratmann RE, Yazyev O, Austin AJ, Cammi R, Pomelli C, Ochterski JW, Ayala PW, Morokuma K, Voth GA, Salvador P, Dannenberg JJ, Zakrzewski VG, Dapprich S, Daniels AD, Strain MC, Farkas O, Malick DK, Rabuck AD, Raghavachari K, Foresman JB, Ortiz JV, Cui Q, Baboul AG, Clifford S, Cioslowski J, Stefanov BB, Liu G, Liashenko A, Piskorz P, Komaromi I, Martin RL, Fox DJ, Keith T, Al-Laham MA, Peng CY, Nanayakkara A, Challacombe M, Gill PMW, Johnson B, Chen W, Wong MW, Gonzalez C, Pople JA (2004) Gaussian 03, Revision D.02. Gaussian, Inc, Wallingford
11. Parr RG, Yang W (1989) Density-functional theory of atoms and molecules. Oxford University Press, New York
12. Becke AD (1993) Density-functional thermochemistry. III. The role of exact exchange. J Chem Phys 98:5648–5652
13. Lee C, Yang W, Parr RG (1988) Development of the Colle-Salvetti correlation-energy formula into a functional of the electron density. Phys Rev B 37:785–789
14. Gonzalez C, Schlegel HB (1990) Reaction path following in mass-weighted internal coordinates. J Phys Chem 94:5523–5527
15. Flükiger P, Lüthi HP, Portmann S, Weber J (2000–2002) MOLEKEL 4.3 Swiss Center for Scientific Computing, Manno. Switzerland
16. Portmann S, Lüthi HP (2000) An interactive molecular graphics tool. Chimia 54:766–770
17. Carpenter JE, Weinhold F (1988) Analysis of the geometry of the hydroxymethyl radical by the "different hybrids for different spins" natural bond orbital procedure. J Mol Struct (THEOCHEM) 169:41–50
18. Foster JP, Weinhold F (1980) Natural hybridorbitals. J Am Chem Soc 102:7211–7218
19. Reed AE, Weinstock RB, Weinhold F (1985) Natural population analysis. J Chem Phy 83:735–746
20. Reed AE, Curtiss LA, Weinhold F (1988) Intermolecular interactions from a natural bond orbital, donor-acceptor viewpoint. Chem Rev 88:899–926

21. Glendening ED, Badenhoop JK, Reed AE, Carpenter JE, Bohmann JA, Morales CM, Weinhold F (2001) NBO 5.0, Theoretical Chemistry Institute, University of Wisconsin, Madison, WI
22. Marten B, Kim K, Cortis C, Friesner RA, Murphy RB, Ringnalda MN, Sitkoff D, Honig B (1996) New model for calculation of solvation free energies: correction of self-consistent reaction field continuum dielectric theory for short range hydrogen-bonding effects. J Phys Chem 100:11775–11788
23. Friesner RA, Murphy RB, Beachy MD, Ringnalda MN, Pollard WT, Dunietz BD, Cao YX (1999) Correlated ab initio electronic structure calculations for large molecules. J Phys Chem A 103:1913–1928
24. Miertus S, Tomasi J (1982) Approximate evaluations of the electrostatic free energy and internal energy changes in solution processes. Chem Phys 65:239–245
25. Bader RFW (1990) Atoms in molecules, a quantum theory; international series of monographs in chemistry, vol 22. Oxford University Press, Oxford
26. Biegler-König F, Schönbohm J, Derdau R, Bayles D, Bader RFW (2002) AIM 2000. Version 2.0, McMaster University